The energy balance in the plasma of a coaxial plasma opening switch

A. Fruchtman[a)]
Center for Technological Education Holon, P.O. Box 305, Holon 58102, Israel

A. A. Ivanov and A. S. Kingsep
Applied Physics Division, Kurchatov Institute, Moscow 123182, Russia

(Received 17 June 1997; accepted 30 December 1997)

The two-dimensional energy flow in the plasma of a coaxial plasma opening switch (POS), during the Hall-induced shock penetration of a magnetic field, is analyzed. The electron collisionality is assumed to be high enough that the dissipated magnetic-field energy becomes electron thermal energy. It is shown that that part of the magnetic-field energy (a third) that is dissipated at the cathode at the generator side of the plasma, becomes an electron kinetic energy, that is convected along the current channel. It is also shown that in the magnetized plasma magnetic-field energy flows *backwards* towards the generator. The third new result is that inside the shock front, electron thermal energy is converted into magnetic-field energy, *contrary* to the usual situation in shock waves in which field energy is converted into particle thermal energy. © *1998 American Institute of Physics.* [S1070-664X(98)01604-8]

I. INTRODUCTION

Magnetic-field penetration into plasma is one of the most fundamental issues in plasma physics. In recent years magnetic-field penetration, which results either from a density nonuniformity or from a cylindrical geometry, has been extensively explored.[1–14] The mechanism of this penetration is of much interest, since it is expected to play a role in processes when the time scale is between the electron and ion cyclotron periods and the length scale is between the electron and ion skin depths. These time scale and length scale are characteristic of plasmas in certain pulsed-power devices, such as the magnetically insulated ion diode (MID),[15] the plasma-filled diode (PFD)[16] and the plasma opening switch (POS),[17,18] and also of some basic plasma physics experiments.[19] Indeed, it has been suggested[2–14] that in short conduction POS experiments[20–23] this mechanism is responsible for the observed fast magnetic-field penetration.[20,22,23]

The electron dynamics and the magnetic-field evolution in the fast processes analyzed here are governed by the equations of electron magnetohydrodynamics (EMH),[1] a branch of multicomponent magnetohydrodynamics (MHD) determined by the condition of smallness of the mass velocity compared to the current velocity. In fact, the ions are assumed here to be immobile. A condition for the validity of EMH is that the characteristic scale of the problem (expressed in terms of gradients) is much smaller than c/ω_{pi}, the ion skin depth. The opposite condition leads to the single-fluid MHD being dominant. We also assume that the electron collisionality is small so that the rate of evolution is not determined by collisional diffusion, but rather by the large Hall electric field.

The penetration of the magnetic field into the plasma must be accompanied by a large magnetic-field energy dissipation. The mechanism of energy dissipation in a low-collisionality plasma is not clear. It has been shown that even if the electron collisionality is low (but not too low), a large dissipation can occur at the shock layer, and the dissipated magnetic-field energy is then converted into electron thermal energy.[4–6] The case of a very low collisionality has also been addressed, and the electron inertia has been shown to be important.[7,9,13,14] The electron temperature was not measured in those recent POS experiments, in which the magnetic-field penetration was measured.[22,23] Future experiments may reveal which process actually dissipates the magnetic-field energy in POS experiments. Theoretical investigations could explore the characteristics of the energy dissipation in the various regimes.

In the present paper we restrict ourselves to the regime in which the electron collisionality is not too low, so that the dissipated magnetic-field energy is converted into electron thermal energy. We present three new results. It has been shown in a two-dimensional (2D) analysis of the energy flow that the magnetic-field energy flux along the current channel near the cathode is only two-thirds of the incoming magnetic-field energy flux in the vaccum.[4] It has been concluded, therefore,[4] that a third of the incoming magnetic-field is dissipated near the cathode at the plasma-vacuum boundary. We show here that this third of the magnetic-field energy, that has been dissipated, is *convected* along the current channel as electron thermal energy. This first new result is derived in Sec. III in which the energy flux along the current channel is analyzed, following the model description in Sec. II. In Secs. IV and V we briefly review the analysis[4] of the energy flow during the Hall-induced shock penetration in a slab geometry, and explain the partition of the energy flow along the current channel. The other two new results concern the evolution of the magnetic field in cylindrical geometry, which we address in Secs. VI and VII. In Sec. VI we analyze the energy flow across the plasma region at the generator

[a)]Electronic mail: fnfrucht@weizmann.weizmann.ac.il

side through which the magnetic field has already penetrated, and present the second new result of the paper: There is a voltage drop from the current layer edge towards the *anode* and the magnetic-field energy flows towards the *generator* in the magnetized plasma. The net magnetic-field energy flux into the plasma, is therefore, *less* than two-thirds of the total energy flux into the plasma. In Sec. VII we examine the energy balance in the shock layer. We show that, contrary to the usual situation, here *at the shock layer electron thermal energy is converted into magnetic-field energy*. This is the third new result of the paper.

II. THE MODEL

The evolution of the magnetic field and the electron dynamics are governed by the EMH equations.[1] The generalized Ohm's law is

$$\mathbf{E}=\eta\mathbf{j}+\frac{1}{nec}\,\mathbf{j}\times\mathbf{B}-\frac{\nabla p_e}{ne}, \tag{1}$$

where the electron inertia is neglected. Also, the processes are so fast that the ions are assumed immobile and the current is due to the electron motion only

$$\mathbf{j}=-en\mathbf{v}_e. \tag{2}$$

Here $\mathbf{E}$ and $\mathbf{B}$ are the electric and magnetic fields, n is the electron density assumed constant in time due to quasi neutrality, e is the elementary charge, η is the assumed small resistivity, v_e is the electron fluid velocity, and p_e is the assumed isotropic electron pressure. The conditions for the electron collisionality which justify the neglect of electron inertia and the assumption of isotropic electron pressure have been discussed before.[4,5] The magnetic-field evolution is determined by Faraday's law

$$-\frac{1}{c}\frac{\partial\mathbf{B}}{\partial t}=\nabla\times\mathbf{E}, \tag{3}$$

where the current and the magnetic field are related by Ampère's law

$$\frac{4\pi}{c}\,\mathbf{j}=\nabla\times\mathbf{B}. \tag{4}$$

The Poynting theorem, that results from Eqs. (3) and (4), is

$$\frac{\partial}{\partial t}\left(\frac{\mathbf{B}\cdot\mathbf{B}}{8\pi}\right)+\frac{c}{4\pi}\,\nabla\cdot\mathbf{E}\times\mathbf{B}=-\mathbf{E}\cdot\mathbf{j}. \tag{5}$$

The electric field energy is smaller than the magnetic-field energy as a result of the neglect of the displacement current in Ampère's law.

The electron pressure p_e is related to the internal electron energy through

$$p_e=\tfrac{2}{3}\epsilon. \tag{6}$$

The electron energy evolution is governed by the electron heat-balance equation

$$\frac{\partial\epsilon}{\partial t}+\nabla\cdot\frac{5}{3}\,\epsilon\mathbf{v}_e=\mathbf{E}\cdot\mathbf{j}, \tag{7}$$

where we neglected the heat conduction. We assume here that $c_P=5/2$ and that $c_V=3/2$. Combining the last two equations, we write the energy conservation as

$$\frac{\partial}{\partial t}\left(\frac{\mathbf{B}\cdot\mathbf{B}}{8\pi}+\epsilon\right)+\nabla\cdot\left(\frac{5}{3}\,\epsilon\mathbf{v}_e+\frac{c}{4\pi}\,\mathbf{E}\times\mathbf{B}\right)=0. \tag{8}$$

In writing Eqs. (7) and (8) we assumed that the electron thermal energy is large compared to the electron kinetic (directed) energy. A condition for the validity of this assumption will be given shortly. Equations (1), (3), and (4) yield the equation that governs the magnetic-field evolution

$$\frac{\partial\mathbf{B}}{\partial t}=\frac{c^2\eta}{4\pi}\,\nabla^2\mathbf{B}-\nabla\times\left(\frac{\mathbf{j}\times\mathbf{B}}{en}\right)+\nabla\left(\frac{c}{en}\right)\times\nabla p_e. \tag{9}$$

In the next section we use the above equations to analyze the energy flow along the current channel.

III. THE CURRENT CHANNEL—THE ENERGY FLOW AND THE VOLTAGE ACROSS IT

We restrict ourselves to configurations in which the magnetic field has one component only, in the ignorable direction. These configurations will be a slab geometry in which the quantities depend on x and z only and the magnetic field has a y component only, and a cylindrical geometry in which the quantities depend on r and z and the magnetic field has a θ component only. We also assume that the density may vary in the direction normal to the electrodes.

A solution of the equations in Sec. II for these configurations shows that the magnetic field may penetrate into the plasma as a shock wave.[1–14] The distribution of the magnetic field in the plasma at a certain time during the shock penetration is shown in Fig. 1 for a slab geometry and in Fig. 2 for a cylindrical geometry. The current flows along the lines in the figures. It is seen that the current flows inside the plasma in a narrow current channel. The current is emitted from the cathode at a small region at the generator edge of the plasma and flows axially along the cathode. It then flows towards the anode at a location that moves axially with the shock propagation.

In this section we calculate the energy flux integrated across the current channel, making use of the fact that the current channel is narrow. Such calculations will be valid for both geometries, and for both current channels, along the cathode and at the shock front. We will then obtain the energy flux per unit length in the ignorable coordinate direction.

Following Eq. (5), the total electromagnetic field flux, the Poynting flux, along the current channel per unit length in the ignorable coordinate direction, is

$$P_{\text{magnetic}}=\frac{c}{4\pi}\int dx_{\text{perp}}\hat{\mathbf{e}}_t\cdot\mathbf{E}\times\mathbf{B}. \tag{10}$$

Also, following Eq. (7) the flux of electron thermal energy is

$$P_{\text{thermal}}=\int dx_{\text{perp}}\hat{\mathbf{e}}_t\cdot\frac{5}{3}\,\epsilon\mathbf{v}_e. \tag{11}$$

In Eqs. (10) and (11) $\hat{\mathbf{e}}_t$ is a unit vector normal to the plane for which we calculate the flux.

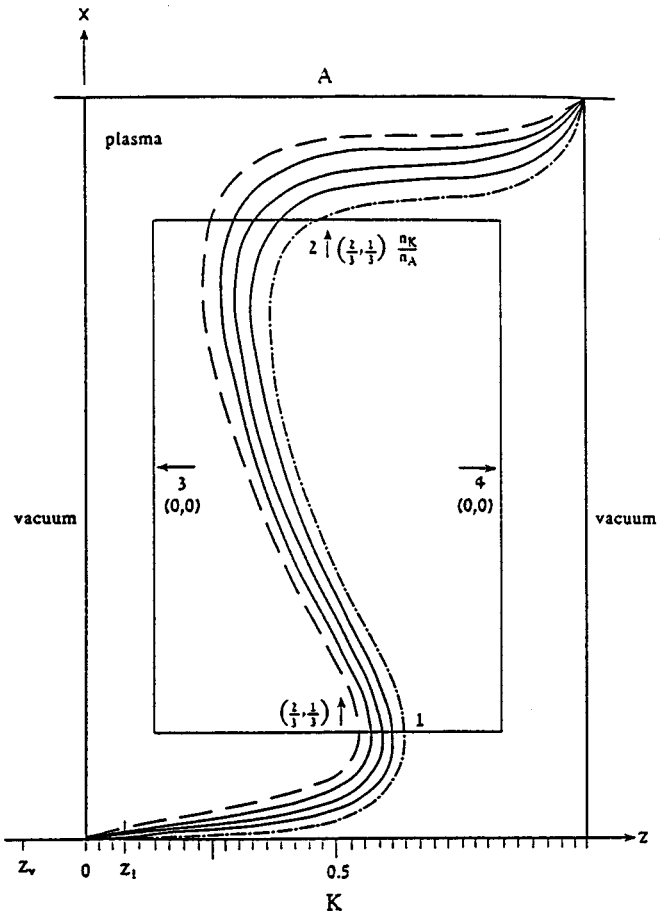

FIG. 1. A slab geometry—the distribution of the magnetic field in the plasma during the shock penetration. The dashed lines are the magnetic-field contours, and also the lines (planes) along which the electron current flows from the cathode (denoted K) towards the anode (denoted A). The region where the dashed lines are is the current channel. The magnetic field is maximal at the generator side of the plasma (to the left of the current channel) and decreases across the current channel. The magnetic field is zero to the right of the current channel. Shown are the values of the energy fluxes through the rectangle boundaries in the directions of the arrows. The first number in each pair is the magnetic-field energy flux and the second number is the thermal energy flux, both in units of $P^{cc}_{total}(z=z_1)$, the total energy flux along the current channel near the cathode.

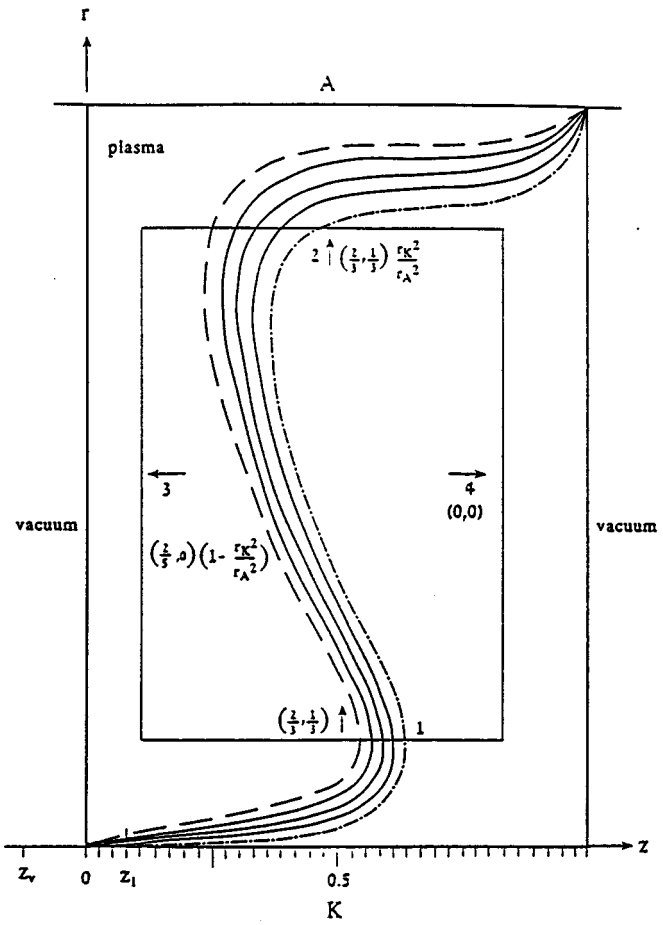

FIG. 2. A cylindrical geometry—the distribution of the magnetic field in the plasma during the shock penetration. The dashed lines are the rB_θ contours, and also the lines (planes) along which the electron current flows from the cathode (denoted K) towards the anode (denoted A). The region where the dashed lines are is the current channel. rB_θ is maximal at the generator side of the plasma (to the left of the current channel) and decreases across the current channel. The magnetic field is zero to the right of the current channel. Shown are the values of the energy fluxes through the rectangle boundaries in the directions of the arrows. The first number in each pair is the magnetic-field energy flux and the second number is the thermal energy flux, both in units of $P^{(cc)}_{total}(z=z_1)$, the total energy flux along the current channel near the cathode.

We assume that the electrons are collisional enough and that the shock penetration is accompanied by a large electron heating. The electron thermal energy is then related to the magnetic field as[5,6]

$$\epsilon = \frac{B^2}{8\pi}. \tag{12}$$

The collision frequency has to be larger than $B/[(8\pi mn)^{1/2}]L$,[4] where L is a characteristic scale length. In this case each electron experiences an average of more than one collision during the time it spends inside the current layer. This collision frequency is much lower than the collision frequency that is needed to explain the fast magnetic-field penetration into the POS plasma. We note that this collisionality, however, is much larger than Spitzer's collisionality. It is comparable to the ion plasma frequency, and may result from the ion acoustic instability.[1]

It is easy to show that, when Eq. (12) holds, the assumption of an electron thermal energy larger than the electron kinetic (directed) energy is justified if the width of the current layer is larger than the electron skin depth, $L \gg c/\omega_{pe}$ (where ω_{pe} is the electron plasma frequency). Together with the usual requirement for the dominance of the Hall field, [1–8] $c/\omega_{pi} \gg L$ (ω_{pi} is the ion plasma frequency), we obtain that our treatment is valid for $c/\omega_{pi} \gg L \gg c/\omega_{pe}$. This regime of validity of the results usually holds for short conduction plasma opening switches.[21]

We calculated the fluxes by performing the integration in Eqs. (10) and (11), using the relations (6) and (12) and the expression for the electric field [Eq. (1)]. We do not show the details of these calculations, which are similar to those performed in Ref. 5. As we mentioned above, we assume that the current channel is narrow so that the plasma density and the coordinates are constant across it. The magnetic field and

the electron pressure do vary, of course, across the current channel.

Integrating Eq. (10) across the current channel we find that the total electromagnetic field flux, the Poynting flux, per unit length in the ignorable coordinate direction through the current channel, is

$$P^{(cc)}_{magnetic}=-\frac{5cB^3_{cc}}{144\pi^2 en_{cc}}. \tag{13}$$

Here n_{cc} is the plasma density at the current channel. This density, uniform across the narrow current channel, may vary along the current channel if the plasma density is not uniform. Also, B_{cc} is the magnetic field at the magnetized side of the current layer. In performing the integrations (10) and (11) we assume that the magnetic field at the cathode side of the current layer is zero. Of the Poynting flux [Eq. (13)] $\frac{3}{5}$ is due to the Hall term and $\frac{2}{5}$ is due to the pressure gradient term in the electric field expression [Eq. (1)]. The electromagnetic flux is mostly magnetic field energy flux, since in the plasma the electric field is much weaker than the magnetic field.

The flux of electron thermal energy is found to be

$$P^{(cc)}_{thermal}=-\frac{5cB^3_{cc}}{288\pi^2 en_{cc}}, \tag{14}$$

where again we used relation (12). The total energy flux through the current channel is the sum of the fluxes given in Eqs. (13) and (14). This sum is

$$P^{(cc)}_{total}=P^{(cc)}_{magnetic}+P^{(cc)}_{thermal}=-\frac{5cB^3_{cc}}{96\pi^2 en_{cc}}. \tag{15}$$

It is clear that the flux of thermal energy [Eq. (14)] comprises a third of the total energy flux in the current channel [Eq. (15)], while the electromagnetic energy flux [Eq. (13)] comprises two thirds of the total energy flux:

$$P^{(cc)}_{magnetic}=\tfrac{2}{3}P^{(cc)}_{total} \tag{16a}$$

and

$$P^{(cc)}_{thermal}=\tfrac{1}{3}P^{(cc)}_{total}. \tag{16b}$$

These relations were noted in Ref. 5 for the energy flow through the current channel at the shock front. As shown here these relations are more general and hold also along the axial current channel near the cathode.

The voltage across the current channel is

$$V^{(cc)}=-\int drE_{perp}=\frac{5B^2_{cc}}{24\pi en_{cc}}, \tag{17}$$

where E_{perp} is the electric field component perpendicular to the current channel. This electric field component, and consequently also the voltage, are also $\frac{3}{5}$ due to the Hall electric field and $\frac{2}{5}$ due to the pressure gradient.

Having derived the above expressions for the voltage across and the energy flux through the current channel, we turn in the next sections to the energy fluxes in the slab and in the cylindrical geometries.

IV. SLAB GEOMETRY—THE AXIAL ENERGY FLOW

We assume that a constant-in-time magnetic field

$$\mathbf{B}=\hat{\mathbf{e}}_y\mathbf{B_0}, \tag{18}$$

that has a y component only, is applied at $z=0$, the plasma—vacuum boundary at the generator side. The cathode is located at $x=0$ and the anode is located at $x=x_A$. For both slab and cylindrical geometry we assume that the cathode and the anode are conductors of infinite conductivity. The plasma density increases monotonically from the cathode towards the anode. The configuration and the resulting magnetic-field distribution at some time after the application of the magnetic field are shown in Fig. 1. We note that in this configuration B_0 is negative.

In the slab geometry the magnetic field, and therefore also the electron pressure, are uniform at the magnetized side of the current channel. As a result the electric field in the plasma is zero except inside the current channel. Therefore, the energy flow through the axial current channel along the cathode and the voltage across it are also the total energy flow inside the plasma between the electrodes and the voltage between them at that axial location.

Following Eqs. (15) and (17), the energy flux per unit length through the plane at z_1, $P^{(KA)}_{total}(z=z_1)$, is

$$P^{(KA)}_{total}(z=z_1)=P^{(cc)}_{total}(z=z_1)=-\frac{5cB^3_0}{96\pi^2 en_K}. \tag{19}$$

The density at the current channel n_{cc} is the density at the cathode n_K since the current channel at $z=z_1$ is in the vicinity of the cathode. Following our analysis of the energy flow along the current channel it is clear that here too the flux of thermal energy comprises a third of the total energy flux in the current channel, while the magnetic energy flux comprises two-thirds of the energy flux

$$P^{(KA)}_{magnetic}(z=z_1)=\tfrac{2}{3}P^{(KA)}_{total}(z=z_1) \tag{20a}$$

and

$$P^{(KA)}_{thermal}(z=z_1)=\tfrac{1}{3}P^{(KA)}_{total}(z=z_1). \tag{20b}$$

The voltage across the electrodes is

$$V^{(KA)}(z=z_1)=V^{(cc)}(z=z_1)=\frac{5B^2_0}{24\pi en_K}. \tag{21}$$

Let us look at the axial energy flux in the vacuum region between the generator and the plasma. The energy flux per unit length in the y direction is

$$P^{(KA)}_{total}(z=z_V)=\frac{c}{4\pi}\int dxE_xB_y=-\frac{c}{4\pi}B_0V^{(KA)}(z=z_V), \tag{22}$$

since the magnetic field in the vacuum is uniform and is given by Eq. (18). The region to the left of the shock front is time independent, and therefore, the voltage between the electrodes at $z=z_V$ is identical to this voltage at $z=z_1$ in the plasma

$$V^{(KA)}(z=z_V)=V^{(KA)}(z=z_1). \tag{23}$$

Substituting expression (21) for the voltage $V^{(KA)}(z=z_1)$ into Eq. (22) we obtain that

$$P^{(KA)}_{\text{total}}(z=z_V)=-\frac{5cB_0^3}{96\pi^2 e n_K}=P^{(KA)}_{\text{total}}(z=z_1). \tag{24}$$

The energy flows from the vacuum into the plasma as an electromagnetic energy at a rate given by expression (24). The energy in the plasma flows at the same rate along the current channel. In the plasma not all the energy flux is electromagnetic energy, a third has been converted into electron thermal energy, as stated in Eq. (20b). The lower rate of magnetic-field energy flow inside the plasma, only two-thirds of the rate in the vacuum, as was noted in Ref. 4, is due to a conversion of a third of the total energy flux into thermal energy flux. This partitioning of energy between magnetic-field energy and electron thermal energy that has been found at the shock layer,[5] exists already in the current channel along the cathode. The dissipated magnetic-field energy, which has been converted into electron thermal energy, is also convected along the current channel as a part of the total energy flux. This is the first new result of this paper.

V. A SLAB GEOMETRY—THE ENERGY FLOW AT THE SHOCK FRONT REGION

The energy flux along the shock front in the slab geometry has been analyzed in Ref. 5. For completeness we briefly present the results here.

The energy flow along the current channel is not constant, since the density varies radially. The net axial flow into a rectangle of a unit length in the y direction is the difference between the inward flow at boundary 1 in Fig. 1 and the outward flow at boundary 2. The fluxes at boundary 1 are

$$P^{(1)}_{\text{magnetic}}=\tfrac{2}{3}P^{(\text{cc})}_{\text{total}}(z=z_1). \tag{25a}$$

$$P^{(1)}_{\text{thermal}}=\tfrac{1}{3}P^{(\text{cc})}_{\text{total}}(z=z_1). \tag{25b}$$

We take boundary 1 to be close enough to the cathode so that the energy flow along the current channel is the same as the energy flow along the current channel near the cathode, and in particular at $z=z_1$. The partition of the flux between magnetic-field energy and electron thermal energy is the same at boundary 2, following our general analysis of the current channel in Sec. III. The fluxes are lower, however, due to the higher plasma density at boundary 2. They are

$$P^{(2)}_{\text{magnetic}}=-\frac{2}{3}\frac{n_K}{n_A}P^{(\text{cc})}_{\text{total}}(z=z_1) \tag{26a}$$

and

$$P^{(2)}_{\text{thermal}}=-\frac{1}{3}\frac{n_K}{n_A}P^{(\text{cc})}_{\text{total}}(z=z_1). \tag{26b}$$

The net magnetic-field energy flux into the region is the sum of the fluxes at the two boundaries. This is because in the slab geometry there is no energy flux through the boundaries 3 and 4. The net magnetic-field energy flux is therefore

$$\Delta P_{\text{magnetic}}=P^{(1)}_{\text{magnetic}}+P^{(2)}_{\text{magnetic}}=\frac{2}{3}\left(1-\frac{n_K}{n_A}\right)P^{(\text{cc})}_{\text{total}}(z=z_1). \tag{27a}$$

Equivalently, the net electron thermal energy flux into that region is

$$\Delta P_{\text{thermal}}=P^{(1)}_{\text{thermal}}+P^{(2)}_{\text{thermal}}=\frac{1}{3}\left(1-\frac{n_K}{n_A}\right)P^{(\text{cc})}_{\text{total}}(z=z_1). \tag{27b}$$

The total energy flux is

$$\Delta P_{\text{total}}=\left(1-\frac{n_K}{n_A}\right)P^{(\text{cc})}_{\text{total}}(z=z_1). \tag{27c}$$

Despite the different rates of flow of the magnetic-field energy and the electron thermal energy, the rates of accumulation of these energies in the plasma are equal. The rate of accumulation of magnetic-field energy in the plasma Q_{magnetic} is

$$Q_{\text{magnetic}}=\int_{x_1}^{x_2}dx\,\frac{B_0^2}{8\pi}\,v_s, \tag{28}$$

where v_s is the shock velocity, the velocity of propagation of the current channel. As was previously shown,[5,6] this velocity is

$$v_s=\frac{5cB_0}{24\pi e}\frac{d}{dx}\left(\frac{1}{n}\right). \tag{29}$$

The rate of accumulation of magnetic-field energy in the plasma is therefore

$$Q_{\text{magnetic}}=-\frac{5cB_0^3}{192\pi^2 e}\left(\frac{1}{n_K}-\frac{1}{n_A}\right)=\frac{1}{2}\left(1-\frac{n_K}{n_A}\right)P^{(\text{cc})}_{\text{total}}. \tag{30}$$

The rate of accumulation of electron thermal energy Q_{thermal} is identical to Q_{magnetic}, because of Eq. (12). Even though the total energy is conserved, as expected, $\Delta P_{\text{total}}=Q_{\text{magnetic}}+Q_{\text{thermal}}$, the net rates of flow of magnetic-field energy and of electron thermal energy are different than the respective rates of accumulation of energy inside the region. This is because inside the shock layer the resistivity cannot be neglected and the work done by the electric field converts magnetic-field energy into electron thermal energy. The work rate, the rate of Joule heating, is found by integration across the region

$$W=\int dz\int_0^{x_A}dx\,\eta j_x^2=\frac{1}{6}\left(1-\frac{n_K}{n_A}\right)P^{(\text{cc})}_{\text{total}}(z=z_1). \tag{31}$$

This is the rate at which magnetic-field energy that flows into the region is converted to electron thermal energy. As was also shown in Ref. 5, this rate is a quarter of the net rate of magnetic-field energy flow into the region [Eq. (27a)]. The rate of accumulation of magnetic-field energy is the net rate of magnetic-field energy flow into the region minus the amount that is being converted to electron thermal energy. Similarly, the rate of accumulation of electron thermal energy is the net rate of electron thermal energy flow into the

region plus the amount that is being converted to electron thermal energy. Using Eqs. (27a), (27b), and (31) we find that these two rates are equal

$$\Delta P_{\text{magnetic}} - W = \Delta P_{\text{thermal}} + W = Q_{\text{magnetic}} = Q_{\text{thermal}}. \tag{32}$$

This makes the total energy accumulated in the plasma equally divided between magnetic-field energy and thermal energy, as also given by Eq. (30).

In the next sections we analyze the cylindrical geometry and present two additional new results.

VI. CYLINDRICAL GEOMETRY—THE AXIAL ENERGY FLOW

Here we assume that a constant-in-time magnetic field

$$\mathbf{B} = \hat{\mathbf{e}}_\theta \frac{b_0}{r}, \tag{33}$$

is applied at $z=0$, the plasma-vacuum boundary at the generator side. The cathode is located at $r=r_k$ and the anode at the larger $r=r_A$. Here $b_0 \equiv r_K B_0$ is constant, and B_0 is the magnetic field near the cathode in the vacuum at the generator side. The plasma density is uniform. The configuration and the resulting magnetic-field distribution at some time after the application of the magnetic field are described by Fig. 2. We note that in this configuration also B_0 is negative. We also note that one can use the relation

$$I = \frac{-cb_0}{2}, \tag{34}$$

between b_0 and the total current I and express the results in terms of I.

The electron thermal energy is

$$\epsilon = \frac{b_0^2}{8\pi r^2}, \tag{35}$$

and the electron pressure is

$$p_e = \frac{b_0^2}{12\pi r^2}. \tag{36}$$

Contrary to the slab geometry, in the cylindrical geometry the magnetic field, and therefore also the electron pressure, are not uniform at the magnetized side of the current channel. As a result the electric field is not zero in the magnetized plasma. Therefore, the voltage between the electrodes falls not only across the current channel, but also across the magnetized plasma, where there is no current. In addition, the presence of an electric field inside the magnetized plasma is accompanied by an energy flow through the magnetized plasma.

Let us first analyze the energy flow through the current channel. In the slab geometry we have written the energy flow per unit length. Here we write the energy flow integrated across the azimuthal direction. Using Eqs. (15) and (17) we find that the energy flow through the current channel at z_1 is

$$P^{(\text{cc})}_{\text{total}}(z=z_1) = -\frac{5cb_0^3}{48\pi e n r_K^2}, \tag{37}$$

and that the voltage across the current channel is

$$V^{(\text{cc})}(z=z_1) = \frac{5b_0^2}{24\pi e n r_K^2}. \tag{38}$$

As has been shown generally in Sec. III, it is easy to show that here too the energy flux through the current channel is divided as two-thirds magnetic-field energy flux and one third thermal energy flux

$$P^{(\text{cc})}_{\text{magnetic}}(z=z_1) = \tfrac{2}{3} P^{(\text{cc})}_{\text{total}}(z=z_1) \tag{39a}$$

and

$$P^{(\text{cc})}_{\text{thermal}}(z=z_1) = \tfrac{1}{3} P^{(\text{cc})}_{\text{total}}(z=z_1). \tag{39b}$$

We also comment that we could define the current channel impedance $Z^{(\text{cc})} = 5I/6\pi e n c^2 r_K^2$ and write the energy flux [Eq. (37)] and the voltage [Eq. (38)] as $P^{(\text{cc})}_{\text{total}}(z=z_1) = Z^{(\text{cc})} I^2$ and $V_0 = Z^{(\text{cc})} I$.

We turn now to the voltage across and the energy flux through the magnetized plasma. The radial variation of the pressure inside the magnetized plasma, according to Eq. (36), is accompanied by the formation of a radial electric field [Eq. (1)]. This radial electric field points inside the plasma in the direction from the cathode to the anode (opposite to the direction the electric field points inside the current channel). Thus, the potential in the magnetized plasma *falls* towards the anode. The potential variation from the cathode to the anode is *nonmonotonic*. The peak of the potential is at the edge of the current channel at the magnetized side. At that axial location the voltage across the current channel is *larger* than the voltage between the electrodes. This voltage across the magnetized plasma, resulting from the pressure gradient, is

$$V^{(\text{plasma})}(z=z_1) = \frac{2}{3}\left(\frac{b_0^2}{8\pi n e r_A^2} - \frac{b_0^2}{8\pi n e r_K^2}\right). \tag{40}$$

Note again that this voltage is *negative*. The voltage between the electrodes at $z=z_1$ is

$$V^{(KA)}(z=z_1) = V^{(\text{cc})}(z=z_1) + V^{(\text{plasma})}(z=z_1). \tag{41}$$

Using the values of the two voltages, Eqs. (38) and (40), we find the voltage between the electrodes at $z=z_1$ to be

$$V^{(KA)}(z=z_1) = \frac{3}{5}\left(1 + \frac{2}{3}\frac{r_K^2}{r_A^2}\right) V^{(\text{cc})}(z=z_1). \tag{42}$$

We note again that the voltage between the electrodes is *smaller* than the voltage across the current channel

$$V^{(KA)}(z=z_1) \leqslant V^{(\text{cc})}(z=z_1). \tag{43}$$

Let us look at the energy flux through the magnetized plasma. All this energy flux is magnetic and therefore

$$P^{(\mathrm{plasma})}_{\mathrm{total}}(z=z_1)=P^{(\mathrm{plasma})}_{\mathrm{magnetic}}(z=z_1)=-\frac{cb_0^3}{24\pi en}\left(\frac{1}{r_A^2}-\frac{1}{r_K^2}\right). \tag{44}$$

Note that the last expression is *negative*. The energy flows in the magnetized region in the direction of the generator. The total energy flux inside the plasma is

$$P^{(KA)}_{\mathrm{total}}(z=z_1)=P^{(\mathrm{cc})}_{\mathrm{total}}(z=z_1)+P^{(\mathrm{plasma})}_{\mathrm{total}}(z=z_1). \tag{45}$$

Using Eqs. (37) and (44) we find the total energy flux between the electrodes at $z=z_1$

$$P^{(KA)}_{\mathrm{total}}(z=z_1)=\frac{3}{5}\left(1+\frac{2}{3}\frac{r_K^2}{r_A^2}\right)P^{(\mathrm{cc})}_{\mathrm{total}}(z=z_1). \tag{46}$$

We note again that the total energy flux is *smaller* than the flux along the current channel

$$P^{(KA)}_{\mathrm{total}}(z=z_1)\leqslant P^{(\mathrm{cc})}_{\mathrm{total}}(z=z_1). \tag{47}$$

At this stage we pause to look at the rate of axial energy flow in the vacuum region between the generator and the plasma. The rate of energy flow in the z direction is

$$P^{(KA)}_{\mathrm{total}}(z=z_V)=P^{(KA)}_{\mathrm{magnetic}}(z=z_V)=\frac{c}{2}\int_{r_K}^{r_A}drrE_rB_\theta=IV^{(KA)}(z=z_V), \tag{48}$$

since the magnetic field in the vacuum satisfies $rB_\theta=b_0$. The region to the left of the shock front is time independent and therefore, as in the slab case, the voltage between the electrodes at $z=z_V$ is identical to this voltage at $z=z_1$ in the plasma, $V^{(KA)}(z=z_V)=V^{(KA)}(z=z_1)$, and therefore

$$P^{(KA)}_{\mathrm{total}}(z=z_V)=\frac{3}{5}\left(1+\frac{2}{3}\frac{r_K^2}{r_A^2}\right)P^{(\mathrm{cc})}_{\mathrm{total}}(z=z_1)=P^{(KA)}_{\mathrm{total}}(z=z_1). \tag{49}$$

The axial energy flows in the vacuum and in the plasma are equal. In the vacuum all the flowing energy is magnetic, while in the plasma part of it is electron thermal energy.

We turn back to the axial energy flow inside the plasma. Let us examine how the energy flux at $z=z_1$ is split between magnetic-field energy and electron thermal energy. The flux of magnetic-field energy is the sum of the positive flux through the current channel [Eq. (39a)] and the negative flux through the plasma [Eq. (44)]

$$P^{(KA)}_{(\mathrm{magnetic})}(z=z_1)=\frac{2}{3}P^{(\mathrm{cc})}_{\mathrm{total}}(z=z_1)-\frac{cb_0^3}{24\pi en}\left(\frac{1}{r_A^2}-\frac{1}{r_K^2}\right). \tag{50a}$$

The thermal energy flows along the current channel only [Eq. (39b)], and therefore

$$P^{(KA)}_{\mathrm{thermal}}(z=z_1)=\tfrac{1}{3}P^{(\mathrm{cc})}_{\mathrm{total}}(z=z_1). \tag{50b}$$

At the limit that $r_K\approx r_A$, both energy flows are mostly through the current channel,

$$P^{(KA)}_{\mathrm{magnetic}}(z=z_1)\approx\tfrac{2}{3}P^{(KA)}_{\mathrm{total}}(z=z_1)$$

and

$$P^{(KA)}_{\mathrm{thermal}}(z=z_1)\approx\tfrac{1}{3}P^{(KA)}_{\mathrm{total}}(z=z_1).$$

Generally, the fraction of the magnetic-field energy flux in the total flux is smaller, and at the opposite limit, when $r_K \ll r_A$

$$P^{(KA)}_{\mathrm{magnetic}}(z=z_1)=\tfrac{4}{9}P^{(KA)}_{\mathrm{total}}(z=z_1) \tag{51a}$$

and

$$P^{(KA)}_{\mathrm{thermal}}(z=z_1)=\tfrac{5}{9}P^{(KA)}_{\mathrm{total}}(z=z_1). \tag{51b}$$

At this limit $P^{(KA)}_{\mathrm{thermal}}(z=z_1)$ is *greater* than $P^{(KA)}_{\mathrm{magnetic}}(z=z_1)$.

Equations (43), (47), and (50a) comprise the main result of this section and the second new result of the paper. The potential does *not* vary monotonically in the radial direction, the magnetic-field energy flows inside the plasma in a direction *opposite* to the direction in which it flows in the current channel, and the fraction of magnetic-field energy flux in the total axial energy flux is *smaller* than inside the current channel, and might be even smaller than the fraction of electron thermal energy flux in the total energy flux.

VII. CYLINDRICAL GEOMETRY—THE ENERGY FLOW AT THE SHOCK FRONT REGION

Let us turn now to the energy balance at the shock front. Similar to what we did for the slab geometry, we look at the energy flow into the segment of the hollow cylinder, the cross section of which is shown in Fig. 2. At the lower boundary 1 energy flows along the current channel. Since this boundary is close to the cathode the energy flux is the same as the energy flux along the current channel at $z=z_1$. The fluxes of magnetic field energy and electron thermal energy are therefore

$$P^{(1)}_{\mathrm{magnetic}}=\tfrac{2}{3}P^{(\mathrm{cc})}_{\mathrm{total}}(z=z_1) \tag{52a}$$

and

$$P^{(1)}_{\mathrm{thermal}}=\tfrac{1}{3}\mathrm{P}^{(\mathrm{cc})}_{\mathrm{total}}(z=z_1), \tag{52b}$$

respectively. The fluxes of energy along the current channel at boundary 2 are

$$P^{(2)}_{\mathrm{magnetic}}=-\frac{2}{3}\frac{r_K^2}{r_A^2}P^{(\mathrm{cc})}_{\mathrm{total}}(z=z_1) \tag{53a}$$

and

$$P^{(2)}_{\mathrm{thermal}}=-\frac{1}{3}\frac{r_K^2}{r_A^2}P^{(\mathrm{cc})}_{\mathrm{total}}(z=z_1), \tag{53b}$$

respectively, where we take boundary 2 to be close to the anode. The partition of the flux between magnetic-field energy and thermal energy is as derived in Sec. III for the current channel. At boundary 2 the fluxes are reduced relative to the fluxes at boundary 1 due to the larger radius. In contrast to the slab geometry, here in the cylindrical geometry there is energy flow in the magnetized plasma through boundary 3. The fluxes through boundary 3 were calculated in the previous section [see Eqs. (37) and (44)]. There is a *backwards* magnetic-field energy flux through the magnetized plasma. Thus

$$P^{(3)}_{\text{magnetic}}=-\frac{2}{5}\left(1-\frac{r_K^2}{r_A^2}\right)P^{(\text{cc})}_{\text{total}}(z=z_1) \tag{54a}$$

and

$$P^{(3)}_{\text{thermal}}=0. \tag{54b}$$

We can now calculate the net energy flux into the region. The net magnetic field and electron thermal energy fluxes are

$$\Delta P_{\text{magnetic}}=P^{(1)}_{\text{magnetic}}+P^{(2)}_{\text{magnetic}}+P^{(3)}_{\text{magnetic}}$$
$$=\frac{4}{15}\left(1-\frac{r_K^2}{r_A^2}\right)P^{(\text{cc})}_{\text{total}}(z=z_1) \tag{55a}$$

and

$$\Delta P_{\text{thermal}}=P^{(1)}_{\text{thermal}}+P^{(2)}_{\text{thermal}}+P^{(3)}_{\text{thermal}}$$
$$=\frac{1}{3}\left(1-\frac{r_K^2}{r_A^2}\right)P^{(\text{cc})}_{\text{total}}(z=z_1). \tag{55b}$$

The net flux of electron thermal energy into the region is *larger* than the net flux of magnetic-field energy, because of the backwards magnetic-field energy flux [Eq. (54a)]. The total net flux of energy into the region is

$$\Delta P_{\text{total}}=\frac{3}{5}\left(1-\frac{r_K^2}{r_A^2}\right)P^{(\text{cc})}_{\text{total}}(z=z_1). \tag{56}$$

The rate of change of the magnetic-field energy inside the region is

$$Q_{\text{magnetic}}=\frac{1}{c}\int_{r_K}^{r_A}dr\,2\pi r\,\frac{b_0^2}{8\pi r^2}\,v_s, \tag{57}$$

where v_s, the shock velocity, is[3–6]

$$v_s=-\frac{cb_0}{4\pi ner^2}. \tag{58}$$

We therefore find that

$$Q_{\text{magnetic}}=\frac{3}{10}\left(1-\frac{r_K^2}{r_A^2}\right)P^{(\text{cc})}_{\text{total}}(z=z_1). \tag{59}$$

Since the density of electron thermal energy in the magnetized plasma is equal to the density of the magnetic-field energy, the rates of accumulation of the two energies are the same

$$Q_{\text{thermal}}=Q_{\text{magnetic}}=\tfrac{1}{2}\Delta P_{\text{total}}. \tag{60}$$

The net flux of energy into the region [Eq. (55)] equals the sum of the rates of accumulation of magnetic field and electron thermal energies in the region [Eqs. (59) and (60)], as it should.

Since the net rate of electron thermal energy flow into the region is larger than the net rate of magnetic-field energy flow into the region, while the rates of accumulation of the two energies are equal, it is clear that in the shock layer electron thermal energy is converted into magnetic-field energy. We show directly that this is indeed the case.

The work done by the electric field on the electrons is composed of Joule heating that converts magnetic-field energy into electron thermal energy and the work done by the electron pressure term

$$\mathbf{E}\cdot\mathbf{j}=\eta j_r^2-\frac{1}{en}\frac{\partial p}{\partial r}\,j_r. \tag{61}$$

Multiplying the r component of Eq. (9) by j_r and integrating over the region in Fig. 2, we find that the Joule heating is

$$\int dz\int_{r_K}^{r_A}dr\,2\pi r\,\eta j_r^2=\frac{1}{10}\left(1-\frac{r_K^2}{r_A^2}\right)P^{(\text{cc})}_{\text{total}}(z=z_1). \tag{62}$$

The electron pressure gradient term converts electron thermal energy into magnetic-field energy:

$$-\int dz\int_{r_K}^{r_A}dr\,2\pi r\,\frac{1}{en}\frac{\partial p}{\partial r}\,j_r=-\frac{2}{15}\left(1-\frac{r_K^2}{r_A^2}\right)P^{(\text{cc})}_{\text{total}}(z=z_1). \tag{63}$$

The net work of the electric field converts electron thermal energy into magnetic-field energy at the rate

$$W=-\frac{1}{30}\left(1-\frac{r_K^2}{r_A^2}\right)P^{(\text{cc})}_{\text{total}}(z=z_1). \tag{64}$$

The difference between the net magnetic-field energy flux into the region and the magnetic-field energy converted into electron thermal energy is easily shown to be equal to the sum of the net electron thermal energy is easily shown to be equal to the sum of the net electron thermal energy flux into the region and the magnetic-field energy converted into electron thermal energy

$$\Delta P_{\text{magnetic}}-W=\Delta P_{\text{thermal}}+W=Q_{\text{magnetic}}=Q_{\text{thermal}}. \tag{65}$$

Equations (62)–(64) comprise the main result of this section and the third new result of this paper. At the shock layer *electron thermal energy is converted into magnetic-field energy*, contrary to the usual case.

VIII. CONCLUSIONS

In this paper we investigated theoretically the energy balance during a fast magnetic-field penetration into a plasma in a plasma opening switch configuration. We assumed that the electron collisionality is low, so that the magnetic-field diffusion is small, but not too low, so that the dissipated magnetic-field energy becomes electron thermal energy. We have shown that that part of the magnetic-field energy (a third) that is dissipated at the cathode at the generator side of the plasma, becomes an electron kinetic energy, that is convected along the current channel. We have also shown that in the magnetized plasma magnetic-field energy flows backwards towards the generator. The third new result is that inside the shock front electron thermal energy is converted into magnetic-field energy, contrary to the usual situation in shock waves in which field energy is converted into particle thermal energy. More experiments are required to find the electron temperature with good spatial and temporal resolutions in order to determine whether the energy

partitioning in POS is as described here. Also, the details of the energy balance during the magnetic-field penetration in the case in which the electron collisionality is too low to cause a large electron heating,[9,13] should be studied theoretically.

ACKNOWLEDGMENTS

The work of A.A.I. and A.K. was supported by Russian Foundation for Basic Research, grant 96-02-16258.

[1] A. S. Kingsep, K. V. Chukbar, and V. V. Yan'kov, *Reviews of Plasma Physics*, edited by B. Kadomtsev (Consultants Bureau, New York, 1990), Vol. 16, p. 243.
[2] A. S. Kingsep, L. I. Rudakov, and K. V. Chukbar, Sov. Phys. Dokl. **27**, 140 (1982).
[3] A. S. Kingsep, Yu. V. Mokhov, and K. V. Chukbar, Sov. J. Plasma Phys. **10**, 1131 (1984).
[4] A. Fruchtman, Phys. Rev. A **45**, 3938 (1992).
[5] A. Fruchtman and K. Gomberoff, Phys. Fluids B **4**, 117 (1992).
[6] A. S. Kingsep and A. A. Sevastyanov, Sov. J. Plasma Phys. **17**, 205 (1991).
[7] Y. L. Kalda and A. S. Kingsep, Sov. J. Plasma Phys. **15**, 508 (1989).
[8] A. V. Gordeev, A. V. Grechikha, A. V. Gulin, and O. M. Drozdova, Sov. J. Plasma Phys. **17**, 650 (1991).
[9] A. Fruchtman and L. I. Rudakov, Phys. Rev. Lett. **69**, 2070 (1992); Phys. Rev. E **50**, 2997 (1994).
[10] J. D. Huba, J. M. Grossmann, and P. F. Ottinger, Phys. Plasmas **1**, 3444 (1994).
[11] R. J. Mason, P. L. Auer, R. N. Sudan, B. V. Oliver, C. E. Seyler, and J. B. Greenly, Phys. Fluids B **5**, 1115 (1993).
[12] P. M. Bellan, Phys. Fluids B **5**, 1955 (1993).
[13] S. B. Swanekamp, J. M. Grossmann, A. Fruchtman, B. V. Oliver, and P. F. Ottinger, Phys. Plasmas **1**, 3556 (1996).
[14] Y. L. Kalda, Phys. Fluids B **5**, 4327 (1993).
[15] R. N. Sudan and R. V. Lovelace, Phys. Rev. Lett. **31**, 1174 (1973).
[16] P. A. Miller, J. W. Poukey, and T. P. Wright, Phys. Rev. Lett. **35**, 940 (1975).
[17] C. W. Mendel, Jr. and S. A. Goldstein, J. Appl. Phys. **48**, 1004 (1977).
[18] P. F. Ottinger, S. A. Goldstein, and R. A. Meger, J. Appl. Phys. **56**, 774 (1984).
[19] R. L. Stenzel, J. M. Urrutia, and C. L. Rousculp, Phys. Fluids B **5**, 325 (1993).
[20] B. V. Weber, R. J. Commisso, R. A. Meger, J. M. Neri, W. F. Oliphant, and P. F. Ottinger, Appl. Phys. Lett. **45**, 1046 (1984).
[21] B. V. Weber, R. J. Commisso, G. Cooperstein, J. M. Grossmann, D. D. Hinshelwood, D. Mosher, J. M. Neri, P. F. Ottinger, and S. J. Stephanakis, IEEE Trans. Plasma Sci. **15**, 635 (1987); H. Bluhm, K. Bohnel, P. Hoppe, H. U. Karow, and D. Rusch, *ibid.* 654; S. Miyamoto, N. Yugami, K. Imasaki, S. Nakai, and C. Yamanaka, *ibid.* 667; A. I. Arbuzov, V. M. Bystritskii, Ya. E. Krasik, V. I. Podkatov, and A. A. Sinebryukhov, *ibid.* 674; Stanley Humphries, Jr., *ibid.* 772.
[22] M. Sarfaty, R. Shpitalnik, R. Arad, A. Weingarten, Ya. E. Krasik, A. Fruchtman, and Y. Maron, Phys. Plasmas **2**, 2583 (1995).
[23] R. Shpitalnik, A. Weingarten, K. Gomberoff, Ya. Krasik, and Y. Maron, Phys. Plasmas **5**, 792 (1998).